Relaxation and Dephasing of Multiexcitons in Semiconductor Quantum Dots

P. Borri, W. Langbein, S. Schneider, and U. Woggon
Experimentelle Physik IIb, Universität Dortmund, Otto-Hahn Strasse 4, D-44221 Dortmund, Germany

R. L. Sellin, D. Ouyang, and D. Bimberg
Institut für Festkörperphysik TU, Hardenbergstrasse 36, D-10623 Berlin, Germany
(Received 15 February 2002; published 10 October 2002)

We measure the dephasing time of ground-state excitonic transitions in InGaAs quantum dots under electrical injection in the temperature range from 10 to 70 K. Electrical injection into the barrier region results in a pure dephasing of the excitonic transitions. Once the injected carriers fill the electronic ground state, the biexciton to exciton transition is probed and a correlation of the exciton and biexciton phonon scattering mechanisms is found. Additional filling of the excited states creates multiexcitons that show a fast dephasing due to population relaxation.

DOI: 10.1103/PhysRevLett.89.187401 PACS numbers: 78.47.+p, 63.22.+m, 78.67.Hc

Semiconductor quantum dots (QDs) are atomlike objects that, with modern nanotechnology, can be fabricated with high crystalline and optical quality. Their application as an active part of novel optoelectronic nanodevices [1] and in quantum information processing [2] is becoming a reality. The knowledge of the homogeneous broadening, inversely proportional to the dephasing time, of an excitonic transition in a QD is of fundamental importance for any of these applications.

Beyond the one exciton limit, multiexcitons in QDs provide additional degrees of freedom for quantum computation [3] and in tailoring quantum devices such as lasers [4] and single photon emitters [5]. The optical properties of multiexcitons in III-V QDs have been addressed experimentally mainly by isolating a single dot from the inhomogeneously broadened ensemble. Pauli blocking allows no more than two carriers in the lowest lying twofold spin degenerate state of electrons (e_0) and holes (h_0), which form the ground-state biexciton. Additional carriers have to occupy higher states. At high exciton occupancies, multiexciton spectra with a large number of emission lines are observed [6] reflecting the renormalization of the transition energies due to Coulomb interaction between carriers [7]. However, the homogeneous broadening of multiexcitonic transitions in QDs was hardly investigated.

We have recently reported on the homogeneous broadening of the transition from the crystal ground state to the e_0h_0 exciton in InGaAs QDs from 7 to 300 K, using a heterodyne four-wave mixing (FWM) technique that allows direct measurement of the dephasing time in an inhomogeneously broadened QD ensemble [8]. The investigated sample was a *p-i-n* ridge waveguide allowing for electrical injection, containing three layers of self-organized $In_{0.7}Ga_{0.3}As$ QDs in the intrinsic region. The measurements were performed without electrical injection in order to investigate the dephasing processes due to exciton-phonon interactions.

In this Letter, we present measurements of the dephasing time of multiexcitonic transitions under electrical injection in the temperature range from 10 to 70 K. By varying the electrical injection we progressively increase the number of excitons in the QDs and investigate the passage from a FWM response dominated by the one exciton transition to a response dominated by multiexcitonic transitions. The measured dephasing is compared with population relaxation dynamics obtained from differential transmission spectroscopy (DTS).

In Fig. 1 a sketch of the investigated structure is shown. In the presence of an injection current (I_C), amplified spontaneous emission spectra are measured (see also Ref. [8]). By comparing with the emission spectra of a sample with twice the length (1 mm), the spectral gain at 10 K was inferred using the stripe-length method [9].

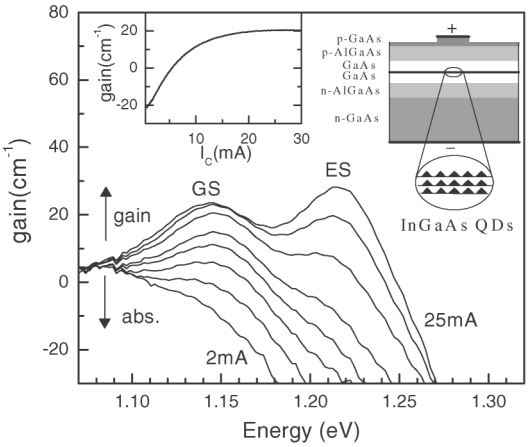

FIG. 1. Spectral gain at 10 K for 2, 4, 6, 8, 10, 15, 20, 25 mA injection current. The inhomogeneously broadened dot ground state (GS) and first optically allowed excited state (ES) transitions are indicated. A sketch of the investigated structure is also shown. In the inset the gain at 1.158 eV is plotted versus injection current.

 0031-9007/02/89(18)/187401(4)$20.00

With increasing I_C the optical response goes from absorption to gain and shows two groups of inhomogeneously broadened transitions labeled GS and ES. The GS group of transitions involves the recombination of e_0h_0 excitons, with or without additional occupation of other dot levels. The ES group involves the recombination of electrons and holes in excited states. Grouped transitions are observed in dots with good cylindrical symmetry [10] where the ES group is dominated by the recombination of electrons and holes in the first two excited levels $e_{1,2}h_{1,2}$. The GS transitions reach transparency (i.e., one e_0h_0 exciton on average) at lower injection current than the ES transitions, and the GS gain saturates for $I_C > 15$ mA (see inset). The FWM experiment is performed using Fourier-limited ~150 fs pulses at 76 MHz repetition rate, with a wavelength of 1070 nm at the center of the GS group, and a heterodyne detection [8]. The pulse intensities excited ~0.1 electron-hole pair per dot, and the FWM signal was in the third-order regime.

The time-integrated FWM field amplitude is shown in Fig. 2 versus the delay time between the exciting pulses at 10 K for different injection currents, as indicated. Without electrical injection ($I_C = 0$), the excitonic transition from the crystal ground state to e_0h_0 (labeled 0-X) is probed in the experiment and shows an initial fast decay followed by a long exponential decay over several hundreds of picoseconds. As discussed in Ref. [8], these dynamics correspond to a non-Lorentzian line shape with a sharp zero-phonon line (ZPL) and a broad band from elastic

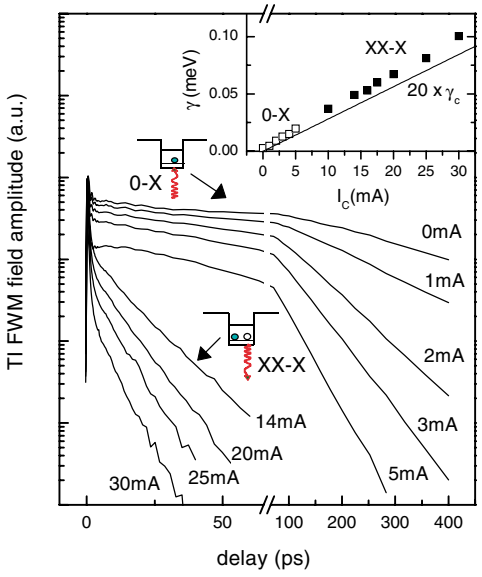

FIG. 2 (color online). Time-integrated four-wave mixing at 10 K and different injection currents, as indicated. The dependence of the homogeneous broadening on injection current deduced from the signal decay at long delays is shown in the inset (squares), together with 20 times the estimated carrier capture rate per dot (line). Sketches of the 0-X and XX-X transitions probed in the experiment are shown (curly arrows are the interacting photons).

exciton-acoustic phonon interaction. At 10 K the ZPL dominates the line shape. With increasing I_C a faster exponential decay of the FWM is observed, i.e., the ZPL broadens due to Coulomb interaction with the injected carriers. For $I_C > 14$ mA, the majority of dots is occupied by two e_0h_0 excitons and the biexciton to exciton transition (labeled XX-X) is probed [11]. The homogeneous broadening of the ZPL shows a linear increase versus I_C (see inset). At low temperature a carrier which is captured into a dot level is not reemitted and changes the oscillation frequency of the GS polarization. As this capture and the subsequent intradot carrier relaxation are statistical processes not linked to the phase of the polarization driven by the laser pulses, they lead to a polarization decay in the measured ensemble average. Thus the capture rate per dot γ_c, which can be estimated using the equilibrium between the total capture rate and the total recombination rate, also leads to a polarization decay rate γ_c. At the transparency current $I_{tr} = 5.5$ mA there is on average one exciton per dot, i.e., the total number of excitons is equal to the number of dots, so that $\gamma_c = \gamma_r I_C/I_{tr}$ using the exciton recombination rate $\gamma_r = 0.67$ μeV obtained from the exciton lifetime of 1 ns measured by DTS [12]. The corresponding homogeneous broadening $2\gamma_c$ is much less than the measured homogeneous broadening due to electrical injection. Electrically injected carriers in the barrier and wetting layer regions thus interact efficiently with the excitonic states in the QD without being captured, and give rise to a pure dephasing of the 0-X and XX-X transitions [14].

By fine variation of the electrical injection near transparency, the passage from a FWM dominated by dots in the 0 state to the one dominated by dots in the XX state occurs. For a dot in the 0 state, the 0-X has a population inversion of -1, while for a dot in the XX state the XX-X transition has a population inversion of $+1$. Therefore, the optically driven polarizations of these two transitions have a relative phase shift of π and thus show a *destructive interference*. This interference is visible in Fig. 3 as a dip in the FWM signal versus delay. If the amplitude of the 0-X and XX-X contributions are similar, which is expected close to transparency, the dip occurs near zero delay. With increasing amplitude of the XX-X contribution the dip shifts to positive delays, as shown in Fig. 3. The rise and decay of the FWM signal after the dip can be fitted by the difference of two exponential decays (dotted line in Fig. 3) and shows that the 0-X transition has a longer dephasing time than the XX-X transition. Since the dephasing of the 0-X and XX-X transitions due to I_C are equal within errors (see slope in the inset of Fig. 2), the difference in the dephasing rates is a sensitive measure of the XX-X dephasing by radiative processes and phonon interaction. In the inset of Fig. 3 the temperature dependence of the 0-X and XX-X ZPL linewidth extrapolated to $I_C = 0$ is shown. The XX-X broadening is larger than the 0-X broadening by a factor that varies with temperature, and tends to one at high

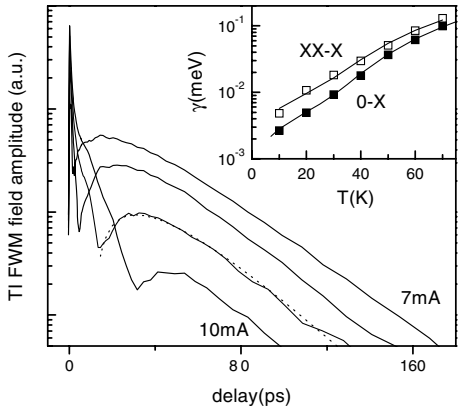

FIG. 3. Time-integrated four-wave mixing at 10 K and 7, 8, 9, 10 mA injection current. The dotted line is a fit to the data at 9 mA. The inset shows the temperature dependence of the 0-X (closed square) and XX-X (open square) homogeneous broadenings for $I_C = 0$, together with fits (solid lines).

temperature. Both dependencies are fitted with the following expression: $\gamma = \gamma_0 + aT + b/[\exp(E_A/kT) - 1]$. We used γ_0 equal to 0.67 and 2 μeV for the 0-X and the XX-X transition, respectively. For the linear temperature dependence we obtain $a_{0-X} = 0.22 \pm 0.02$ μeV/K and $a_{XX-X} = 0.37 \pm 0.04$ μeV/K. The thermally activated behavior is identical within error for both transitions, with an activation energy $E_A = 16 \pm 1$ meV and $b = 1.1 \pm 0.2$ meV. $\gamma_0 = 0.67$ μeV is taken from the measured exciton lifetime of 1 ns and 2 μeV, i.e., 3 times this value, for the XX-X transition corresponds to a fully uncorrelated radiative decay of the three involved excitons. If a_{0-X} is due to transitions between the different spin states of the e_0h_0 exciton as we suggested in Ref. [8], a_{XX-X} and a_{0-X} should be equal, since XX is a singlet spin state. Alternative explanations could be the broadening of the ZPL due to the elastic exciton-acoustic phonon interaction expected if virtual excitations of the excited states or a finite phonon lifetime are considered. Finally, the activated part of the 0-X broadening was attributed to a phonon-assisted transition of the e_0h_0 into the e_0h_1 exciton state [8]. The identical activated part of the XX-X transition indicates fully correlated exciton and biexciton scattering via phonon absorption, similar to observations in InGaAs/GaAs and GaAs/AlGaAs quantum wells [15] and in CdSe/ZnSe quantum dots [16].

With increasing electrical injection above 15 mA, saturation of the e_0h_0 excitons and filling of the $e_{1,2}h_{1,2}$ excitons occurs (see Fig. 1). In the presence of $e_{1,2}h_{1,2}$ excitons the probed GS transition in the FWM experiment goes from a multiexciton ground state to a multiexciton excited state with only one e_0h_0 exciton. This transition has a strong final state damping due to the relaxation of the excited multiexciton into its ground state with two e_0h_0 excitons, resulting in a fast FWM decay (see fast initial dynamics for $I_C > 15$ mA in Fig. 2). We have probed this relaxation dynamics in a degenerate DTS experiment on the GS transition utilizing the same heterodyne technique as the FWM experiment. A strong pump pulse leads a weak probe at positive delay time, and the heterodyne detection selects the transmitted probe instead of the FWM signal [17]. DTS data were taken for varying I_C from 0 to 30 mA.

The pump-induced change of the gain, deduced from the probe differential transmission, is shown in Fig. 4 at 10 K for transparency of the GS transition ($I_C = 5.5$ mA) and strong filling of the $e_{1,2}h_{1,2}$ excitons ($I_C = 30$ mA). In a QD ensemble, a macroscopic configuration for a given electrical injection is a superposition of microstates [13]. A microstate of a QD is defined by the occupation of the dot levels with integer numbers of carriers. The probability of finding a specific microstate in the macroscopic configuration depends on I_C. Each microstate has a given internal dynamics while only the capture rate is proportional to I_C. Good fits to the DTS data required at least four time constants. In Fig. 4 the fourfold exponential fit function has been decomposed into the contributions for the different time constants, to explain the role of different microstates in the DTS signal. Moreover, an instantaneous contribution from nonresonant two-photon absorption and coherent artifacts was included [17]. The amplitudes $A_1 \ldots A_4$ of the time constants versus

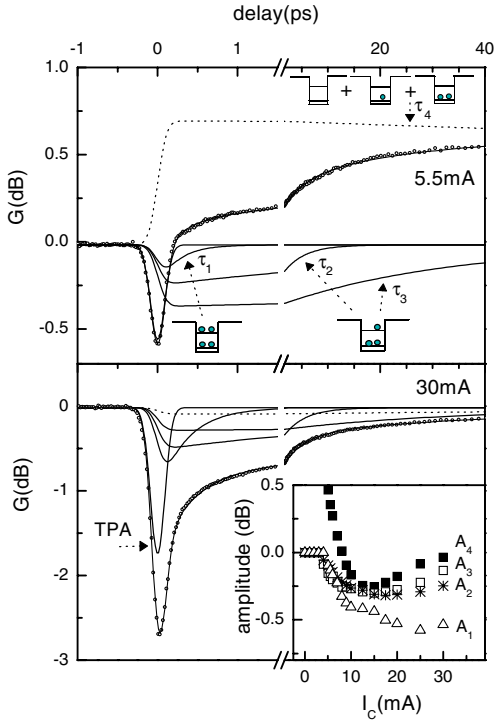

FIG. 4 (color online). Differential transmission spectroscopy at 10 K and different injection currents, as indicated. The measured change of the gain in decibels is shown (open circles) together with its best fit (solid line). A decomposition of the fit into four exponential contributions, and an instantaneous response from two-photon absorption (TPA) is also shown. In the inset the dependence of the amplitudes of the four exponential contributions versus injection current is shown.

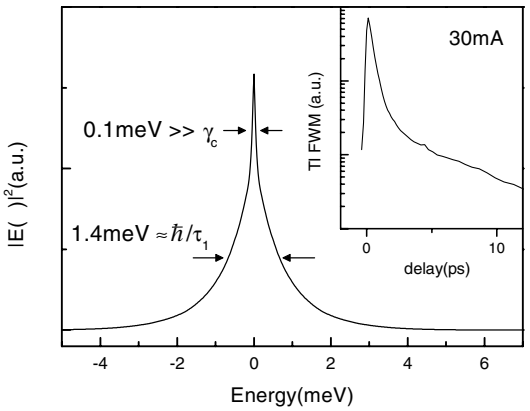

FIG. 5. Power spectrum of the four-wave mixing field amplitude at 30 mA and 10 K. The full widths at half maximum of the two Lorentzian contributions to the line shape are indicated. In the inset the initial fast dynamics of the four-wave mixing versus delay time is given.

injection current are shown in the inset of Fig. 4. All the microstates recover, after the interaction with the pump photons and the internal relaxation dynamics, on a long time scale, determined by the interplay between radiative recombination and capture [13], represented by τ_4 which varies from 1 ns to 200 ps going from $I_C = 0$ to 30 mA. At low temperature before the optical excitation, the carrier configuration of each microstate is in its ground state (see sketches in Fig. 4). Microstates with no carriers in the excited states do not have internal relaxation dynamics and thus evolve only with τ_4. After the removal of a e_0h_0 by the pump photons, microstates with a high number of carriers in the excited states undergo a fast relaxation dynamics, modeled by $\tau_1 = 0.33 \pm 0.05$ ps, due to the high number of final states available for the phonon-assisted relaxation. However, microstates with only one carrier in the first excited state have only one relaxation channel. We suggest that the slow time constants $\tau_2 = 4 \pm 0.3$ ps and $\tau_3 = 35 \pm 4$ ps refer to this relaxation for a hole or an electron. This is supported by the fact that A_2 and A_3 have similar values versus I_C, as expected from the overall charge neutrality of the dot ensemble.

We can finally compare the measured relaxation dynamics of the multiexcitons with the FWM decay. From the inset of Fig. 4 we observe that at 30 mA the DTS response is dominated by the microstates with more than one carrier in the excited states, thus allowing for a simple comparison between the measured time constant τ_1 and the FWM decay. Apart from the initial rise, the time-integrated photon echo versus delay is a probe of the time evolution of the first-order polarization and its Fourier transform is similar to the homogeneous line shape [8]. In Fig. 5 the calculated power spectrum of the TI FWM field amplitude at 30 mA is shown with a zoom of the FWM versus delay time in the inset. The line shape of the power spectrum is well represented by a sum of two Lorentzians, with the widths indicated in the figure. The sharp Lorentzian is the Fourier transform of the long exponential decay, corresponding to the broadening of the XX-X transition due to pure dephasing from the injected carriers in the barriers. Conversely, the width of the broad Lorentzian corresponds to the broadening given by τ_1, showing that the dephasing of the probed multiexcitonic transition is dominated by population relaxation.

In conclusion, we found that electrically injecting carriers decreases the dephasing time of excitonic transitions in InGaAs quantum dots at low temperature. In particular, a pure dephasing due to carriers injected in the barrier material and a dephasing of multiexcitonic transitions by population relaxation are distinguished. These results might be of considerable importance for future applications based on a coherent optical control of the excitonic transitions in quantum dots and suggest that barrier engineering could reduce the dephasing time by one order of magnitude to the limit given by the capture rate. Additionally, the temperature dependent dephasing of the biexciton to exciton transition revealed an exciton and biexciton correlated phonon scattering, which should stimulate further theoretical work.

This work was supported by DFG (Wo477/17-1 and SFB296). P. B. is supported by the European Union (MCFI-2000-01365).

[1] D. Bimberg, M. Grundmann, and N. N. Ledentsov, *Quantum Dot Heterostructures* (John Wiley and Sons, Chichester, 1999).
[2] Pochung Chen, C. Piermaroccchi, and L. J. Sham, Phys. Rev. Lett. **87**, 067401 (2001).
[3] Filippo Troiani, Ulrich Hohenester, and Elisa Molinari, Phys. Rev. B **62**, R2263 (2000).
[4] Y. Z. Hu, H. Giessen, N. Peyghambarian, and S. W. Koch, Phys. Rev. B **53**, 4814 (1996).
[5] D. V. Regelman *et al.*, Phys. Rev. Lett. **87**, 257401 (2001).
[6] E. Dekel *et al.*, Phys. Rev. Lett. **80**, 4991 (1998).
[7] A. J. Williamson, A. Franceschetti, and A. Zunger, Europhys. Lett. **53**, 59 (2001), and references therein.
[8] P. Borri *et al.*, Phys. Rev. Lett. **87**, 157401 (2001).
[9] C. B. à la Guillaume, J.-M. Debever, and F. Salvan, Phys. Rev. **177**, 567 (1969).
[10] M. Bayer *et al.*, Phys. Status Solidi (b) **224**, 331 (2001).
[11] O. Stier *et al.*, Phys. Status Solidi (b) **224**, 115 (2001).
[12] The estimated rate assumes capture of electron-hole pairs. Independent capture of electrons and holes does not substantially modify this estimate (see Ref. [13]).
[13] M. Grundmann and D. Bimberg, Phys. Rev. B **55**, 9740 (1997).
[14] A. V. Uskov *et al.*, Appl. Phys. Lett. **79**, 1679 (2001).
[15] P. Borri, W. Langbein, J. M. Hvam, and F. Martelli, Phys. Rev. B **60**, 4505 (1999); W. Langbein and J. M. Hvam, Phys. Rev. B **61**, 1692 (2000).
[16] F. Gindele, K. Hild, W. Langbein, and U. Woggon, Phys. Rev. B **60**, R2157 (1999).
[17] P. Borri *et al.*, Appl. Phys. Lett. **79**, 2633 (2001).